Powered Engine Simulator Procedures and Experience for the DC-10 Wing Engine

H. R. WELGE* AND J. R. ONGARATO†
Douglas Aircraft Company, Long Beach, Calif.

The techniques and experience in using a powered engine simulator to evaluate nacelle performance and engine installation effects are described. A three-phase test program of calibration, isolated-nacelle testing, and wing-nacelle testing is described. Basic engine performance, in the form of a compressor map, compressor and turbine efficiency, and swirl is shown. Methods of model design, the isolated-nacelle model support system, external-flow effects on discharge coefficient, and a method of obtaining an evaluation of interference effects are considered. Additional results shown pertain to the elimination of ice formation on the gas-generator surface due to the low-temperature turbine exhaust air. Also, results of thrust similarity of various engines are discussed. The use of the simulators for evaluation of in-flight thrust is discussed briefly.

Nomenclature

A	=	area
C_d	=	airplane drag coefficient, drag/$q_0 A_{\text{wing}}$
C_D	=	nozzle discharge coefficient, $W_{A\text{ACT}}/W_{A\text{IDEAL}}$
C_L	=	airplane lift coefficient, lift/$q_0 A_{\text{wing}}$
C_P	=	pressure coefficient, $(P - P_0)/q_0$
C_T	=	gross thrust coefficient, ($F_{g\text{ACT}}$ − NACELLE DRAG)/$F_{g\text{IDEAL}}$
D	=	diameter
F_g	=	gross thrust
F_N	=	net thrust
L	=	length
M	=	Mach number
N	=	rotor speed, revolutions/min
P	=	static pressure
P_T	=	total pressure
$P_T/P)_{\text{CAL}}$	=	fan-exhaust-nozzle calibration pressure ratio
q	=	dynamic pressure, $(\gamma/2)PM^2$
T_T	=	total temperature, °R
W_A	=	airflow, lb/sec
V	=	velocity
X	=	linear distance
γ	=	ratio of specific heats
δ	=	$P/2116$, P units lb/ft²
δ_T	=	$P_T/2116$, P_T units lb/ft²
θ_T	=	$T_T/519$, T_T units °R

Subscripts

FAN	=	fan exhaust
MAX	=	maximum
0	=	freestream
REF	=	reference conditions
TD	=	turbine drive nozzle
TED	=	turbine exhaust nozzle

Introduction

CURRENT high-subsonic-speed transport-aircraft engines with a front fan and a short-duct nacelle have the high-velocity fan exhaust located very close to the lower surface of the wing. The fan nozzle is usually choked and operates at a pressure ratio near three. Therefore, there is an over-expansion of the jet flow and a compression-expansion cycle following the nozzle exit. The pressures produced by this compression-expansion cycle can interact with the low-pressure, high-velocity region under the wing to produce supersonic velocities and even lower pressures. Since the pressure must rise to ambient, a shock wave can form, producing drag. A way of evaluating these phenomena is to use a powered engine simulator, like the one shown in Fig. 1, to measure the variation of airplane lift and drag with nozzle pressure ratio when the engine is installed under the wing. The force measurements, together with pressure distributions on the nacelle-pylon-wing combination, allow an assessment of the acceptability of the design. Using powered engine simulators is preferred to placing a high-pressure air-supply pipe under the wing, a technique which could produce unrealistic flowfields. Also, the boundary layer in the critical regions between the wing and nacelle is closely simulated

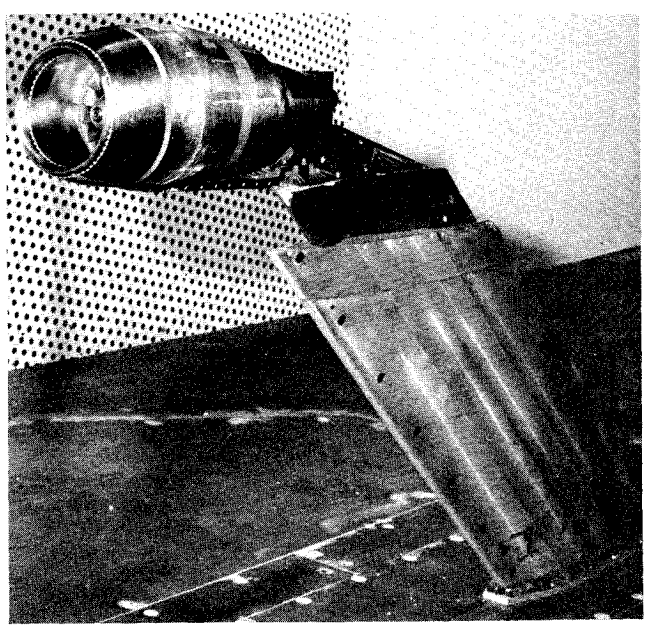

Fig. 1 Cornell installation.

Presented as Paper 70-590 at the AIAA 5th Aerodynamics Testing Conference, Tullahoma, Tenn., May 18–20, 1970; submitted June 12, 1970; revision received December 10, 1970.

* Senior Engineer Scientist, Aerodynamics Section Advanced Technology and Development Branch.

† Senior Engineer Scientist, Aerodynamics Section Wind Tunnel Test Branch.

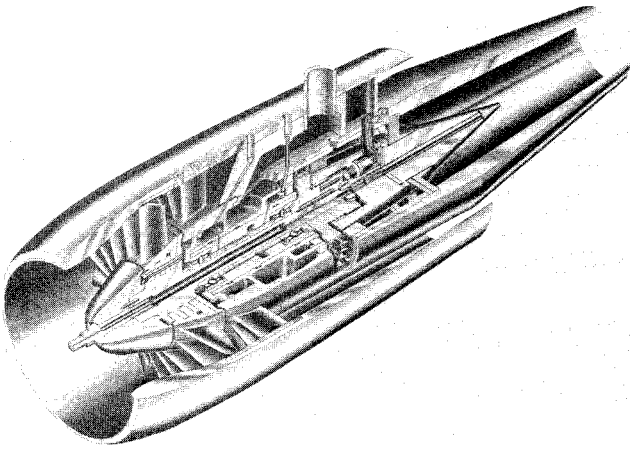

Fig. 2 Powered simulator.

by the powered simulator. This is important, since afterbody separations for a given configuration are affected by the state of the boundary layer as well as by the nozzle pressure ratio.

The nacelle by itself must have acceptable performance. The acceptability of the nacelle design is assessed by testing the isolated nacelle-pylon (isolated from the wing flowfield). With the engine simulator operating, comparison of the experimental simulator thrust and the predicted thrust indicates the acceptable performance of the nacelle.

Another use of the engine simulator is to evaluate the influence of external flow on nozzle performance. The engine manufacturer runs the actual engine on a thrust stand without any external flow and without the presence of the wing. The effects of the external flow on the engine can be assessed by comparing the performance of the powered simulator when tested with and without external flow. Any adverse effects on engine performance or on thrust can be determined

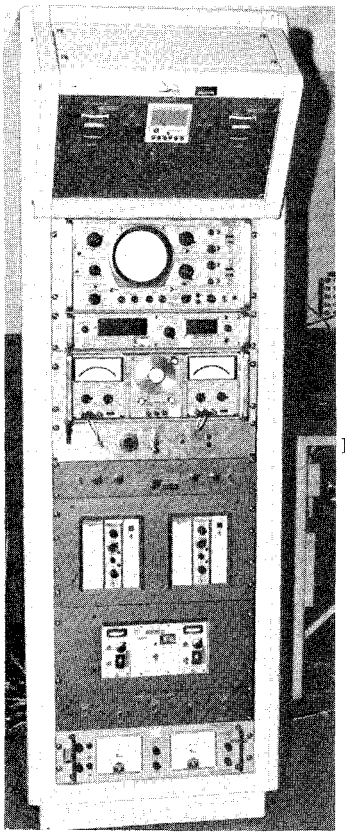

Fig. 3 Engine control console.

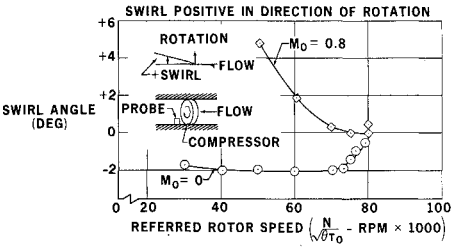

Fig. 4 Swirl at compressor exit.

before flight test, allowing the design to be changed early in the program.

Powered Simulator

The air-driven eingine simulator, shown in Figs. 1 and 2, was designed by Pratt & Whitney and built by the Tech Development Company. An air-driven, single-stage turbine powers a single-stage compressor (nitrogen instead of air has also been used). At the design condition of 80,000 rpm, the turbine operates with a drive pressure of about 350 psi, and the fan develops a total-pressure rise of about 1.60. The maximum diameter of the fan case is 4.1 in., and the ratio of the compressor diameter to the turbine diameter is about the same as that of the full-scale engine, so that the fan duct and the external gas-generator surface can be accurately simulated.

In the construction of the inlet cowl, the aft fan cowl, and the turbine gas generator, "O" rings were used to ensure an airtight assembly of the engine nacelle. A filter capable of handing 10-μ particles and larger was used in the turbine-drive air-supply system to prevent erosion of the turbine-bucket leading edges. The rotating parts of the engine are supported on two oil bearings, each of which has its own annular oil tank to provide four hours of running time between oil refills.

The McDonnell Douglas Corporation has five of these powered simulators that have been used in the wind-tunnel testing program for the DC-10 airplane. A total running time of 780 hr has been accumulated. Approximately 70% of the running time has been at 70,000 rpm and higher. Currently, one of the simulators has accumulated 228 hr of running time.

Engine Control System

The engine control system (shown in Fig. 3) provides complete remote control of the powered engine by scheduling the turbine-air-supply throttling valve. The throttling valve incorporates a servo system that maintains a constant preselected air-supply rate to the engine. The console also monitors and visually displays rpm of the engine, engine-bearing temperatures, and throttling-valve position and incorporates oscilloscopes for measuring engine vibration and engine shaft run-out. Through preselected limit controls, automatic shutdown will occur if the upper limit of any of the previous parameters is exceeded.

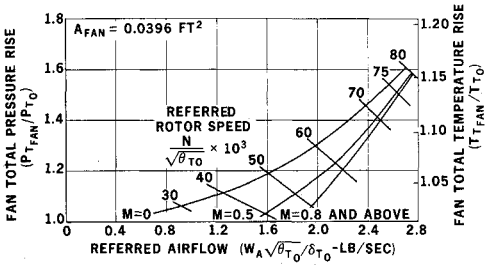

Fig. 5 Fan map.

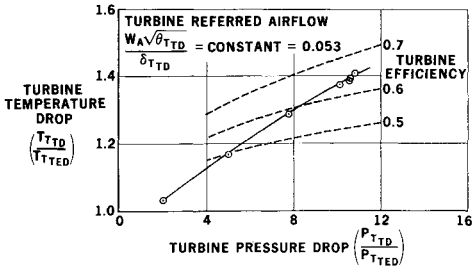

Fig. 6 Turbine efficiency.

Model Instrumentation

The powered engine nacelle model was instrumented with 267 pressure taps on the pylon, external fan cowl, gas-generator surface, and internal fan and turbine sections. Sixteen total-head tubes and eight static-pressure taps were located just downstream of the fan. Four static-pressure taps were located near the fan-nozzle exhaust section. Twelve total-head tubes were located in the engine turbine section. The gas-generator external surface was instrumented with 60 static-pressure taps. The external fan cowl contained 60 static-pressure taps, and the pylon was instrumented with 107 static-pressure taps. A pressure tube was also provided in the engine-turbine plenum chamber.

The engine contained four thermocouples in the fan section, four in the turbine section, and two thermocouples each for the front and rear bearing. The engine also had two speed sensor pickups.

Test Procedure

The following procedure is suggested to evaluate nacelle performance and wing installation effects. Actual data obtained during the DC-10 test program are used to illustrate the procedures. Test facilities used were the Cornell Aeronautical Lab 8-Foot Transonic Tunnel,[1] the United Aircraft Subsonic 8-Foot Tunnel‡ and the Douglas Aircraft Company Aerophysics Lab.§

A test procedure for determining interference effects should be divided into three phases. The first phase is concerned with calibrating the fan airflow. The airflow calibration is used in later phases to determine the effect of external flow on the fan discharge coefficient. The airflow calibration is also used in later test phases to determine the engine gross thrust from net-force measurements. During the initial calibration, other engine-monitoring parameters, such as turbine efficiency, fan efficiency, and turbine-drive-nozzle airflow, are determined.

The second phase is an isolated test in which the complete nacelle is tested in the presence of external flow but not in the

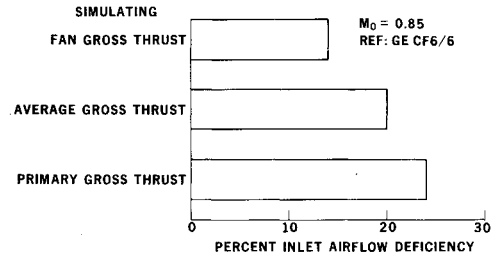

Fig. 7 Airflow deficiency with thrust simulation.

‡ The United Aircraft Research Laboratory Subsonic Wind Tunnel; United Aircraft Corporation; East Hartford, Conn.

§ The Douglas Aerophysics Laboratory, McDonnell Douglas Corporation; El Segundo, Calif.

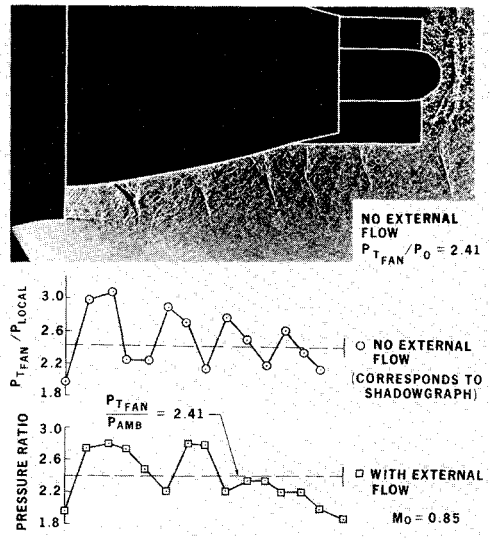

Fig. 8 Shadowgraph of nozzle flow—$P_{T_{FAN}}/P_0$ = 2.41.

presence of the wing. The isolated thrust coefficients (the quotient of actual gross thrust and ideal gross thrust) and the effects of external flow on discharge coefficient are determined.

The isolated thrust coefficients are used in the third phase in which the nacelle and the wing are tested together. The difference between the wing-engine forces with power and the wing-engine forces without power is compared to the thrust increment predicted from the isolated-nacelle testing. If the installed increment agrees with the isolated increment, the effects of power are small and the design is acceptable. Pressure distributions on the wing-nacelle-pylon combination are also considered in the assessment of the acceptability of a particular design. Most nacelle-placement studies are done with flow-through nacelles, which are less costly, simpler, and more sensitive to small changes in drag. Therefore, the no-power case relates to the flow-through nacelle testing, and the effects of power can be evaluated as increments to the no-power case.

First Phase—Calibration

The fan airflow is calibrated in a test rig where the area behind the fan can be evacuated to any pressure and atmospheric pressure acts in front of the fan. The area downstream of the fan is evacuated so that the nozzle pressure ratios of high Mach numbers can be duplicated. There is no external flow over the model during this calibration. (The effect of external flow is evaluated in the second phase by comparing the fan discharge coefficients at the same nozzle pressure ratio.)

The fan exhaust duct contains total-pressure, static-pressure, and total-temperature instrumentation. The instrumentation is necessary for two reasons: first, to determine the airflow in the fan duct by calibration and second, to determine the fan-exhaust total pressure.

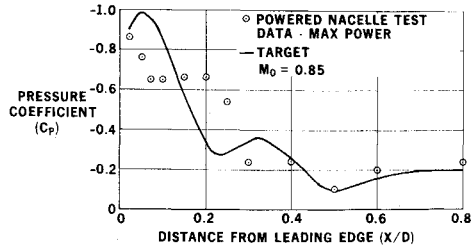

Fig. 9 Inlet external flow simulation.

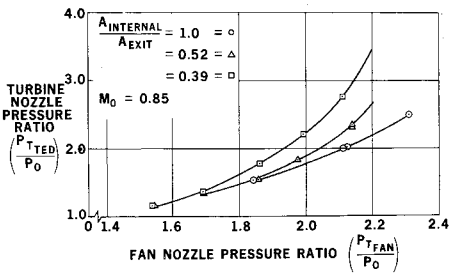

Fig. 10 Effect of turbine-exhaust internal blockage on nozzle pressure ratios.

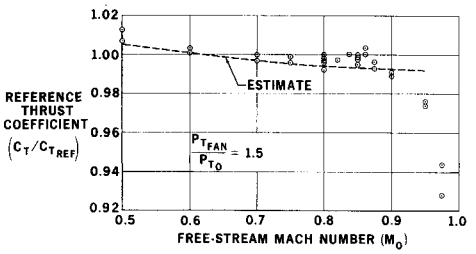

Fig. 12 Variation of thrust coefficient with Mach number—isolated nacelle.

The referred airflow in the fan-exhaust duct is calibrated against the quotient of the fan-exhaust total pressure and the local static pressure at the rakes. If the flow is one-dimensional, this relationship is unique [i.e., the referred airflow is only a function of the ratio $P_T/P)_{CAL}$]. However, because of swirl in the fan flow and the way it shifts with rotor speed (Fig. 4), the instrumentation is not adequate to give an accurate calibration. Therefore, the referred rotor speed must be introduced as another parameter. The airflow is then calibrated with pressure ratio and rotor speed. In performing the calibration, all these quantities are measured. During the external-flow testing, $P_T/P)_{CAL}$ and the rotor speed are measured and the airflow determined from the calibration curve. If the external flow reduces the amount of airflow at a given nozzle pressure ratio, the ratio $P_T/P)_{CAL}$ will respond to this suppression, and the effects of external flow on the fan discharge coefficient can be determined. The turbine airflow is determined from an orifice meter located in the control system of the high-pressure turbine-supply system.

During this testing phase, the parameters are determined that are used to monitor engine performance and to ensure that the instrumentation is functioning properly throughout the remaining phases. These parameters are the fan map and efficiency, the turbine efficiency, and the turbine drive-nozzle referred airflow. (The turbine referred airflow is a constant, since the turbine drive nozzle is always choked.) Typical values of these parameters are shown in Figs. 5 and 6.

The airflow entering the inlet of the simulator is always deficient relative to the full scale engine, because the air that drives the turbine and leaves the turbine nozzle enters from an external source. So, if the fan-nozzle area is simulated, the airflow entering the inlet for any fan pressure ratio will be deficient by $1/(1 + BPR)$, where BPR is the bypass ratio. The airflow deficiencies incurred while simulating the fan gross thrust, the turbine gross thrust, and the average gross thrust are shown in Fig. 7.

A shadowgraph of the fan nozzle flow without external flow is shown in Fig. 8. The pressure distributions shown on the lower part of the figure indicate how the shock wave pattern changes with external flow. (Shadowgraph pictures with external flow were not obtained).

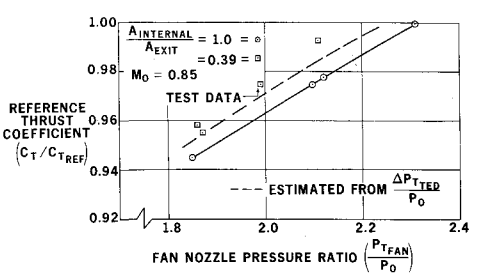

Fig. 11 Effect of turbine-exhaust internal blockage on thrust coefficient.

Second Phase—Isolated Nacelle With External Flow

The nacelle is mounted in the tunnel and tested at various nozzle pressure ratios in the presence of external flow. The method of supporting the nacelle-pylon model is important. Two bodies in close proximity to each other in a subsonic airstream will exert mutual, equal and opposite pressure forces. But there will be no net pressure force as stated by d'Alembert's paradox. If one of the bodies is grounded (not on the balance system) and the other is on the balance system (metric), an unrealistic force will be experienced by the balance. Therefore, near the body the support system has to be metric. Since the pressure forces between the metric support and the metric nacelle-pylon are equal and opposite, there is no net pressure force and it is correct to test the support alone without the nacelle-pylon attached and subtract this force from the nacelle-pylon-support force.

At a certain distance from the nacelle and low subsonic airflows, the pressure forces, produced by the nacelle-pylon, are negligible and the support can be made nonmetric from that point to the wall. In transonic flow, pressure disturbances will go all the way to the wall. But if the support were made metric to the wall, the drag of the support system, which must be removed from the balance force to obtain the desired nacelle and pylon drag, becomes large compared to the model force desired. Therefore, the pressures produced by the nacelle, when integrated over the frontal area of the nonmetric portion of the support, should be small when compared to the balance accuracy. These pressures can be estimated from potential-flow solutions with the appropriate corrections for compressibility. For the testing considered here, the support was metric to 1.25 nacelle diameters from the nacelle centerline. This resulted in a small remaining body-produced pressure force and a ratio of metric-support wetted area to model wetted area that amounted to 30%. The support is shown in Fig. 1.

An advantage of the aforementioned procedure is that any extraneous forces in the balance system are automatically removed. The extraneous force will be in both the nacelle-pylon-support data and in the support-alone data. When the support-alone force is subtracted from the total nacelle-pylon-support force, the extraneous force is eliminated.

The incoming momentum of the turbine air should be properly removed from the net force of the nacelle. The momentum of the wall-support system can be eliminated by bringing the air across the balance system in a direction perpendicular to the freestream flow.

The nacelle afterbody should be built to exactly duplicate the actual engine nacelle externally and to duplicate it internally aft of the exhaust total-pressure instrumentation.

Because no freestream air passes through the turbine, the inlet mass flow will always be less for the model than for the actual engine at the same exhaust-nozzle conditions (Fig. 7). The result of the decreased mass flow is greater negative pressures on the forebody of the nacelle. The cowl-forebody lines should be modified by reducing the highlight diameter enough to make the cowl-forebody peak pressure and drag characteristics similar to those of the actual engine cowl.

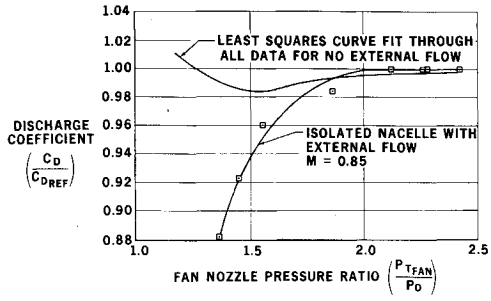

Fig. 13 Effect of external flow on fan discharge coefficient.

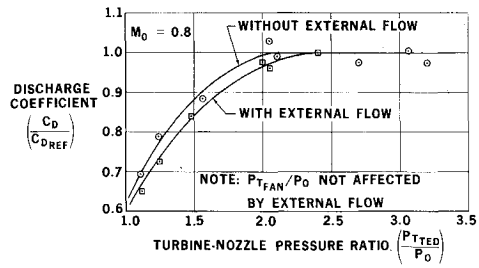

Fig. 14 Effect of external flow on turbine nozzle discharge coefficient.

An indication of the cowl flow simulation obtained during the current test is shown in Fig. 9.

The isolated-nacelle model should not be contoured to the airplane flowfield. Testing a contoured nacelle in the uniform flowfield would give unrealistic nacelle drag. A contoured nacelle in a uniform flowfield has inlet contours that are locally too thin or too thick and boattail angles that are locally too large or too small, compared to the flowfield of the actual nacelle on the airplane. Also, a contoured nacelle has induced drags in the uniform flowfield of isolated testing that do not exist in the airplane flowfield. This will result in apparent, favorable interference effects. A properly contoured nacelle operating in the airplane flowfield should have essentially the same drag as an axisymmetric nacelle operating in the uniform flowfield of the wind tunnel. Any drag increment due to improper contouring appears as interference drag and should be considered an installation effect. Also, for similar reasons, the nacelle drag should be measured only at zero degrees angle of attack. Any incremental drag incurred as a result of changes in the local angle of attack of the installed nacelle is considered to be an installation effect.

Blockage in the turbine exhaust duct can be used to produce a range of turbine-nozzle pressure ratios at a given fan-nozzle pressure ratio. A range may be necessary, since the relation between the two pressure ratios may produce thrust differences in different test phases that need to be accounted for. This was investigated experimentally during the testing. It can be shown analytically that, if the turbine does a constant amount of work, and the turbine exhaust nozzle is choked, increased pressure loss in the turbine exhaust stream will result in increased turbine exhaust-nozzle pressure. Also, the pressure loss is only a function of the ratio of the area at the blockage to the exhaust area. Figure 10 indicates the results obtained by reducing the flow area upstream of the exhaust nozzle to 52% and to 39% of the exhaust area. Figure 11 shows the resulting increase in the thrust coefficient. This increase is predictable to $0.005C_T$.

The point of boundary-layer transition on the model should be fixed. If transition is not fixed, the point of natural transition can move unrealistically as the Mach number is increased. Also, the point of natural transition may not be the same in various test phases, since the model may be tested in different tunnels with different turbulence levels. For the DC-10 nacelle, 0.003-in.-thick triangular tape was used and placed 0.1 in. from the leading edge externally and 0.3 in. internally (Fig. 1).

An example of isolated thrust coefficients is shown in Fig. 12. These thrust coefficients were obtained with the model shown in Fig. 1. The extended support pylon was tested alone, and its drag was removed from the data obtained for the configuration shown in Fig. 1. The value of C_T was computed from

$$C_T = (F_{BAL} + F_{RAM})/(F_{gFANI}C_{DFAN} + F_{gPRII}C_{DPRI})$$

where F_{BAL} is the balance force, corrected for the isolated support drag; F_{RAM} is the ram drag (product of the fan airflow determined from the calibration and the tunnel velocity); F_{gFANI} and F_{gPRII} are the fan and turbine ideal gross thrust, respectively; and C_D is the nozzle discharge coefficient.

The value of the discharge coefficient is computed for each data point. The product of the discharge coefficient and the ideal gross thrust is equal to the product of the actual airflow and the nozzle ideal velocity. The equation for the ideal gross thrust is derived from

$$F_{gi} = (\rho_a A V_a) V_i$$

where ρ_a is the theoretical density at the nozzle exit, A is the nozzle geometric area, V_a is the theoretical velocity at the nozzle exit, and V_i is the ideal velocity when the airflow is expanded to ambient pressure.

The isolated thrust coefficients will be used later in the installed phase to give the predicted force change. Note that the variation of thrust coefficient in Fig. 12 follows the estimated variation, which is calculated from nozzle performance and skin friction.

An example of the effect of external flow on the discharge coefficients is shown in Figs. 13 and 14. The fan airflow was obtained from the calibration curve, and the turbine airflow was metered in the supply system. Here we see a large effect due to external flow when the nozzles are unchoked. This effect is due to the higher than ambient pressures at the nozzle exit and to the contraction of the exhaust-flow streamlines outside of the nozzle caused by the momentum of the external flow into the nozzle stream.

Third Phase—Installed Test

The simulator is placed under the wing, and the combination is tested at various Mach numbers and lift coefficients. The engine fan total-pressure ratio is set at unity (known from the isolated testing), and the airplane drag polar is recorded. The power is then increased (to maximum in this case) and the airplane drag polar recorded again (Fig. 15). The increment in airplane drag then is compared to the increment predicted from the isolated data at the same nozzle pressure ratio. If there are no effects of power, these values will

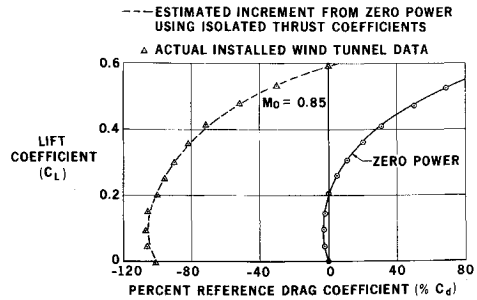

Fig. 15 Evaluation of interference effect.

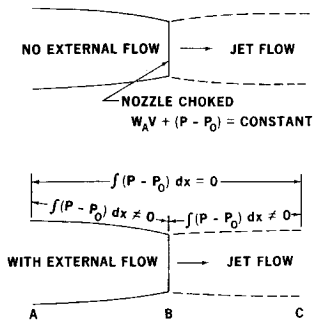

Fig. 16 Nozzle-exhaust thrust change with external flow.

agree, as shown on Fig. 15. However, if there is an adverse interference effect, the drag of the complete airplane will be greater than the value predicted from the isolated data. As was mentioned, this procedure lends itself to the development testing with flow-through nacelles.

The engine should be run with no external flow when installed under the wing. The forces measured then should be compared to the isolated thrusts with no external flow, to make sure that the effects of a new tunnel installation are not affecting the balance force.

The method previously described considers only the effects of power on the engine installation. The effects of power, as well as changes in external drag, can be evaluated by taking the force from the isolated-wing data (no engine) and adding to it the thrust predicted by the isolated engine. The sum is compared to the thrust of the wing-engine combination, and the interference force evaluated. This procedure has been tried by Patterson[2] and is acceptable if the wing installation is unchanged from wing-along to wing-engine tests. The problem with the procedure is that, if the wing data are taken from a previous test, the isolated wing-data can be slightly different when the new installation is made, and this distorts the interference effects.

In-Flight Thrust

The engine manufacturer runs the full-scale engine on the thrust stand without any external flow. If the full-scale engine cannot be run with external flow because of its large size, the powered simulator can be used. It can be run in such a way that the results will be analogous to the results for the full-scale engine, and it can also be run with external flow. The differences between the data with and without external flow can be applied to the full-scale engine data to account for the effects of external flow. An assessment of the thrust increment is needed to properly determine the airplane drag, since the engine thrust in level, steady flight is equal to the airplane drag. Unlike the blown-pipe system, this system has no boundary-layer problem. Here again, screens can be used to vary the ratio of fan to turbine-nozzle pressure, so that the effect of unsimulated turbine-nozzle pressures can be evaluated. Also, unrealistic swirl properties of the powered simulator are eliminated, since only increments are used.

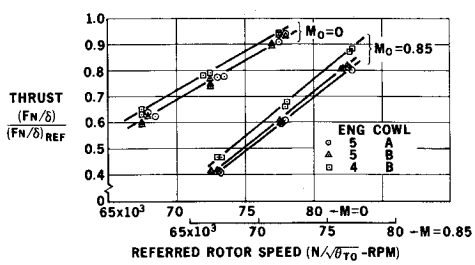

Fig. 17 Thrust variation between cowls and engines.

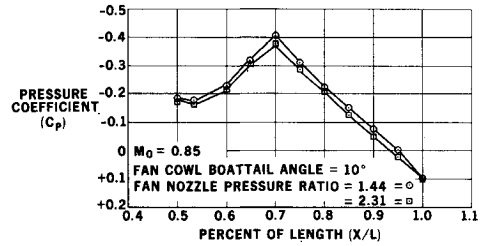

Fig. 18 Effect of power on fan-cowl-afterbody pressures.

It is necessary to test with external flow because forces are introduced which can not be estimated with accuracy. The flow changes the engine force by an amount equal to the skin friction drag on the external surface. In addition, there is an incremental pressure force on the body produced by the interaction of the external flow and the jet. The occurrence of the incremental pressure force can be illustrated by considering a nonviscous potential flow over the body shown in Fig. 16. The nozzle is choked and the momentum at the nozzle exit plane is the same with or without external flow. With no external flow there will be no pressure force on the external surface and the force will be that produced by the nozzle momentum. However, with external flow there will be a nonzero pressure force on the body (represented by the force from A to B in Fig. 16) because the pressure force from upstream to downstream infinity must be zero (A to C in Fig. 16).

Additional Items Concerning Model Testing

The temperature drop in the turbine is sufficient to cool the outer gas-generator surface to the point where the moisture in the fan flow condenses and forms ice. Running for long periods (15–30 min) would cause a considerable amount of ice to form on the surface, making the model unacceptable for testing. Of the methods of eliminating the ice formation that were tried, the best was to heat the turbine-drive air. The turbine-drive air temperature required depended on the amount of moisture and the temperature of the fan flow. If 70°F atmospheric air is drawn through the fan, the turbine-drive air temperature required is about 160°F. Running at Cornell with a tunnel total temperature of 110°F and dry tunnel air, only 110°F turbine-drive air temperature was required. There were no detrimental effects on the engine.

The problem arises, in testing an airplane with more than one engine, as to whether all the engines need to be calibrated for forces. Referring to Fig. 17, we see that there was a 5% difference between two engines tested in the same cowl. However, the same engine in two different cowls produced very little difference. (The cowls were built to the same lines but were different pieces of hardware.) Therefore, the data indicated that, once an engine has been calibrated, it may be assumed to have the same characteristics in a similar cowl, but that each engine has to be calibrated for accurate force measurements.

The effects of high nozzle pressure ratios on the fan-cowl-afterbody pressure distribution with the thin boundary layers (compared to blown-pipe testing) are small, as is indicated in Fig. 18. These data were for a 10° boattail angle. Smaller boattail angles (3°) tend to be affected more by the nozzle pressure ratio.

Conclusions

1) The testing technique is considered successful (Figs. 12 and 15). 2) The effects of external flow on fan and turbine discharge coefficient can be properly evaluated (Figs. 13 and 14). 3) The modification of the inlet cowl to account for the

reduced airflow prevented early drag rise of the model (Fig. 9). 4) Blockage in the turbine exhaust is effective in changing the relationship between the primary and fan nozzle pressure ratio (Figs. 10 and 11). 5) Gas-generator surface ice was eliminated by heating the turbine-drive air. 6) Each engine needs to be calibrated for force (Fig. 17).

References

[1] "The Cornell Aeronautical Laboratory 8-Foot Transonic Wind Tunnel," WTO-300, Nov. 1964, Cornell Aeronautical Lab., Buffalo, N.Y.

[2] Patterson, J. C., "A Wind Tunnel Investigation of Jet Wake Effect of High-Bypass Ratio Engine on Wing-Nacelle Interference Drag of a Subsonic Transport," TN D-4693, 1968, NASA.

JULY 1971 J. AIRCRAFT VOL. 8, NO. 7

DC-10 Test Program Effectiveness

ARTHUR TOROSIAN* AND JAMES F. MURRAY†
Douglas Aircraft Company, Long Beach, Calif.

The DC-10 aircraft test program has been planned to provide increased over-all efficiency and effectiveness. A series of comprehensive engineering development simulations and aircraft ground tests will precede the flight test program, which will employ a sophisticated data acquisition and processing system with the capability to provide real-time data while the tests are in progress. A flight controls development test stand will be used to evaluate the prototype flight control and avionic equipment and provide the capability for pilot assessment of the Flight Guidance and Control (FG&C) System by means of an integrated simulator complex. A laser beam tracking system will be used to provide the space positioning data required in Flight Guidance and Control, noise measurement, and takeoff and landing performance tests. Training on the DC-10, which began one year prior to the scheduled first flight, will be broadened to include test runs and flight simulation to establish plans and to train all test-related personnel.

Introduction

A DEFINITION of the DC-10 test program effectiveness is presented in this paper as the efficient planning, instrumentation, execution, and analysis of engineering development simulator tests and airplane ground and flight tests to, 1) evaluate aircraft performance and flying qualities, 2) define the operational envelope, 3) evaluate systems performance, and 4) demonstrate that the aircraft and its systems comply with airworthiness standards established by applicable Federal Aviation Regulations (FAR).

As the nature and scope of aircraft testing in a general sense are well established, only aspects of testing that are innovations or otherwise uniquely related to recent aircraft design changes or test techniques and those related to changes in the Federal Aviation Administration (FAA) certification requirements are discussed in this article. Most considerations of test effectiveness presented herein are applicable to large-scale test programs on any model of commercial or military aircraft; however, because of the author's more recent experience, specific details refer to the DC-10 aircraft test program.

General

The growth of commercial aviation from its initial stages has been phenomenal as a result of public acceptance of air travel and advances in aircraft technology and design. Aircraft have increased in size, flight envelopes have grossly expanded, systems have become more sophisticated, and although costs per seat or ton mile have gone down, flight test costs have gone up. As a result of these factors, it is necessary to conclude that laboratory simulation and development and prototype ground testing must be comprehensive and effectively programed to reduce flight test requirements and in turn provide for an accelerated and efficient flight test program.

Test Planning Concepts

The initial consideration necessary to achieve an effective test program is the planning phase wherein the over-all test program must be prepared to achieve the following objectives:

Conduct an efficient and safe envelope expansion program and qualitatively and quantitatively evaluate the design flight characteristics, structural integrity, system functions, aircraft performance, and operational suitability of the aircraft and its associated equipment.

Establish configuration improvements as required during the flight test program and qualify those changes in the initial stages of test to ensure compliance with the delivery schedules.

Demonstrate the aircraft and its systems in accordance with applicable Federal Aviation Regulations and customer contractual requirements.

In the DC-10 test program, as an important part of the over-all planning effort, a comprehensive program of laboratory and ground tests was established to precede the flight test program. The technical details of this rigorous program of functional and environmental testing will contribute to minimize flight test problems. In addition, the major system integration simulators will remain active during flight test to assist in the resolution of problems discovered in flight. Laboratory and Flight Development organizations that are responsible for the ground and flight testing facilities and all test functions have been integrated to provide the means for efficient conduct of the over-all DC-10 test program. An integrated organization of this kind ensures that data are efficiently exchanged and that flight test personnel will be

Presented as Paper 70-371 at the AIAA Test Effectiveness in the 70's Conference, Palo Alto, Calif., April 1-3, 1970; submitted April 20, 1970; revision received October 2, 1970.

* Engineering Test Pilot. Member AIAA.

† Manager, DC-8/DC-9 Flight Test. Associate Member AIAA.